JOURNAL OF CATALYSIS 126, 555–571 (1990)

Oxidation of Carbon Monoxide over Palladium on Zirconia Prepared from Amorphous Pd–Zr Alloy

I. Bulk Structural, Morphological, and Catalytic Properties of Catalyst

A. BAIKER,*,[1] D. GASSER,* J. LENZNER,* A. RELLER,† AND R. SCHLÖGL‡

*Department of Industrial and Engineering Chemistry, Swiss Federal Institute of Technology, Eidgenössische Technische Hochschule Zentrum, CH-8092 Zurich, Switzerland; †Institute of Inorganic Chemistry, University of Zurich, CH-8057 Zurich, Switzerland; and ‡Fritz Haber Institute der Max Planck Gesellschaft, 1000 Berlin 33, Federal Republic of Germany

Received May 9, 1990; revised July 11, 1990

Catalysts highly active for the oxidation of carbon monoxide have been prepared by oxidation of amorphous and crystalline Pd_1Zr_2 metal alloys. The oxidation was carried out *in situ*; i.e., the fresh metal alloys were exposed to CO-oxidation conditions at temperatures of 473–553 K. Under these conditions, the initially almost inactive metal alloys underwent a series of solid state reactions and were finally transformed into stable and highly active microporous catalysts. Bulk structural characterization using X-ray diffraction and electron microscopy revealed that the final catalysts were made up of small intergrown and poorly crystalline domains of different palladium and zirconia phases. Palladium was present in three forms in the active catalysts, as a solid solution of palladium and oxygen, as metallic palladium, and as PdO. Zirconia existed in monoclinic and tetragonal forms. Comparative kinetic measurements carried out in a differential fixed bed reactor in the temperature range 300–500 K indicated that the activity of the palladium species in the catalysts derived from the metal alloys was more than an order of magnitude higher than the activity of the palladium species in a palladium on zirconia catalyst prepared by impregnation. The comparison of the activities was based on turnover frequencies calculated on the basis of accessible palladium sites determined by CO chemisorption. The higher activity of the catalysts derived from the metal alloys is attributed to their unique structural and chemical properties leading to extremely large interfacial areas and possibly to enhanced oxygen transfer via the solid–solid interphase.

INTRODUCTION

Oxidation of carbon monoxide to carbon dioxide by oxygen is still the most efficient method of removing highly diluted carbon monoxide from gaseous wastes. The most common catalysts used for this reaction are the oxides of several transition metals as well as noble metals on supports. Numerous studies on this reaction with supported and pure noble metals (Pt, Pd, Ir, Ru, Rh) have been performed in the past. The results of earlier work on the catalytic oxidation of carbon monoxide on platinum metals have been reviewed by Engel and Ertl (*1*).

Amorphous metal alloys have gained considerable interest as model catalysts due to their unique structural and chemical properties (*2*). Recently, particular emphasis has been devoted to their use as catalyst precursors. The progress in this research has been reviewed very recently (*3, 4*). Various supported metal catalysts have been prepared by pretreatment or *in situ* activation from amorphous metal alloys. Under appropriate conditions the amorphous metal alloys can undergo a series of solid state reactions which finally yield supported metal catalysts

[1] To whom correspondence should be addressed.

0021-9517/90 $3.00

with unique structural and morphological properties. The oxidic support may be formed by selective oxidation of the more electropositive constituent(s) of the alloy. This process can lead to phase separation and excessive crystallization of the metal in metal/metalloid alloys, as has been shown for several zirconium-containing alloys (*5*). As-prepared catalysts have been applied so far predominantly for reactions carried out under reducing conditions (*3, 4, 6*); i.e., for hydrogenation reactions.

We have reported recently in a preliminary communication (*7*) that highly active CO-oxidation catalysts could be prepared from an amorphous Pd_1Zr_2 metal alloy by *in situ* activation, i.e., by exposure of the alloy to CO oxidation conditions. The turnover frequencies referred to the palladium atoms were considerably higher in as-prepared catalysts then in a conventionally prepared zirconia supported palladium catalyst measured under the same conditions.

The aim of the present work is to gain insight into the complex physical and chemical changes which occur in the bulk and surface of the amorphous precursor during its transition to the active catalyst. In this paper, we focus on the changes of the bulk structure and surface morphology of the precursor alloys during activation and their influence on the development of the catalytic activity of these materials. X-ray diffraction (XRD), differential thermal analysis (DTA), thermogravimetry (TG), gas adsorption measurements, scanning electron microscopy (SEM), and high-resolution electron microscopy (HREM) are used to pursue this aim. The changes in the surface chemical properties of the alloy and their influence on the mechanism of the CO oxidation will be addressed in part II (*8*) of this series.

EXPERIMENTAL

Catalysts

The amorphous Pd_1Zr_2 used as catalyst precursor was prepared from the premixed melt of the pure metals by rapid quenching using the technique of melt spinning. Chemical bulk analysis by means of inductive coupled plasma (ICP) and X-ray fluorescence (XRF) revealed that the final alloy contained traces (ppm level) of Hf, Cu, and Si besides the main constituents. For use in the catalytic tests, the 5 mm wide and 20–30 μm thick ribbons fabricated by the melt spinning were ground to flakes of 0.1–1 mm size under liquid nitrogen. X-ray diffraction indicated that the ground material was still completely amorphous. Amorphous and crystalline Pd_1Zr_2 alloys were used as catalyst precursors. Crystalline Pd_1Zr_2 alloy was obtained from amorphous Pd_1Zr_2 by annealing it at 870 K in vacuum. As reference catalysts, palladium-on-zirconia catalysts which contained 1 and 5 wt% of palladium were prepared by impregnation of ZrO_2 with an aqueous solution of $(NH_4)_2PdCl_4$ using the incipient wetness technique. Subsequent to drying for 12 h at 390 K, the precursor was calcined and reduced under a flowing hydrogen–nitrogen mixture ($H_2 : N_2 = 1 : 10$) for 15 h at 470 K, 1 h at 570 K, and finally 1 h at 670 K. High-resolution transmission electron microscopy and X-ray analyses indicated that the catalyst prepared by impregnation consisted of Pd particles supported on crystalline zirconia adopting mainly the baddeleyite structure (*9*).

Catalyst Characterization

The precursor materials and the final catalysts were investigated with regard to their physical and chemical properties using X-ray diffraction (XRD), differential thermal analysis (DTA), thermogravimetry (TG), gas adsorption (N_2, CO, and krypton), scanning electron microscopy (SEM), and high-resolution electron microscopy (HREM).

CO chemisorption measurements were used to evaluate the number of surface palladium atoms. Prior to CO adsorption measurements, the samples were reduced in pure hydrogen at 493 K for 12 h and subsequently evacuated (10^{-4} Pa) at the same temperature for 24 h. CO adsorption measurements were carried out at 300 K and

included the subsequent steps; (i) measurement of total CO uptake corresponding to strongly and weakly adsorbed CO; (ii) evacuation of the sample for 1 h at 10^{-4} Pa; (iii) measurement of CO uptake corresponding to weakly adsorbed molecules. The amount of chemisorbed CO was calculated as the difference of the two adsorption uptakes. In the literature (*10, 11*) values between 1 and 2 are reported for the stoichiometric factor Pd_S/CO of CO chemisorption, depending on the prevalence of linear or bridge-bonded CO on the surface. CO chemisorption studies have so far mainly been carried out on either pure palladium powder or silica and alumina supported palladium. Studies of the CO adsorption using diffuse reflectance FTIR spectroscopy (*12*) revealed that on the catalysts prepared from the Pd–Zr alloys bridge-bound CO was the prevalent surface species in a pure CO atmosphere. Based on this observation the palladium surface area was estimated assuming a stoichiometric factor of two for the CO chemisorption and a cross-sectional area of 7.87×10^{-20} m^2 for the palladium atom (*13*). The dispersion D of the palladium was calculated as $D = Pd_s/Pd_{total}$, where Pd_s corresponds to the number of palladium surface metal atoms and Pd_{total} to the total number of palladium atoms in the sample.

X-ray diffraction was used for qualitative phase analysis and the determination of the mean crystallite sizes of the constituents. X-ray diffraction patterns were obtained using a powder diffractometer under the following conditions: Cu$K\alpha$, 25 mA, 40 kV, Ni-filter, $\lambda = 1.5406$ A; goniometer speed 0.5° (2θ)/min.

Estimates of the mean crystallite size d_{hkl} were made using the width of selected diffraction peaks at half maximum and the Scherrer equation $d_{hkl} = 51\ \lambda/(B \cos \theta)$, where d_{hkl} is the mean crystallite size in angström units, and B the observed peak width at half maximum peak height. As the value of B is influenced by instrumental factors as well as crystallite size effects, corrections concerning the instrumental broadening and $K\alpha$-doublet broadening were made according to the procedure described in Ref. (*14*).

Scanning electron microscopy (JEOL JSM 840) was used to investigate the grain morphology of the samples. High-resolution electron microscopy and selected area electron diffraction were carried out using a JEOL 200CX microscope equipped with top entry stage. The materials were gently ground and dispersed in hexane. The slurry was disposed on a copper grid covered with a holey film of amorphous carbon. Optical diffraction patterns of selected domains were obtained using a He/Ne laser installed on a standardized optical bench.

Catalytic Tests

Kinetic measurements were carried out using an apparatus which consisted of an isothermal continuous fixed bed reactor, the gas dosing and purification, and two IR analyzers for the measurement of CO and CO_2, respectively. The Pyrex glass reactor was 30 cm long and had an inner diameter of 1 cm. The temperature in the catalyst bed was measured by a thermocouple, which was inserted in the center of the bed. The reactor temperature could be held within ±1 K. Reactant gases were taken from pressure gas cylinders in which the gases CO (99.99%)/N_2 (99.995%) and O_2 (99.999)/N_2 (99.995%) were premixed. The reactant feed rate was controlled by mass flow controllers (Brooks). The concentration of CO and CO_2 were measured at the reactor inlet and outlet, respectively. Comparative activity tests were carried out under the following conditions: temperature range, 300–500 K; partial pressure; CO, 0.17 kPa; O_2, 0.17 kPa; total pressure, 100 kPa; balance gas, N_2; total flow rate, 2.5 cm^3/s (STP); catalyst load, 0.3 g. The catalyst grain size used for the catalytic tests was 50–150 μm.

The kinetic experiments were started by heating the catalysts in the reactant gas mixture to the temperature where the *in situ* activation was carried out. This temperature was used as reference temperature to check whether the catalyst maintained stable ac-

tivity during the series of kinetic measurements. After kinetic measurement at a given temperature the catalyst was again heated up to the reference temperature to confirm that the activity remained stable during the kinetic measurements.

Preliminary tests using different flow rates, while the ratio of catalyst weight to molar flow rate was kept constant, indicated that the flow rate used (2.5 cm^3/s) in the kinetic tests was large enough to avoid any influences caused by nonideal flow patterns (back-mixing) and/or interparticle mass and heat transfer limitations. The absence of intraparticle mass transfer influences was evidenced for the conventionally prepared catalysts by carrying out kinetic runs with different catalyst particle sizes. Similar tests with regard to intraparticle mass transfer influences could not be performed with the catalysts derived from the PdZr alloys since the particle size could not be varied in a sufficiently large range due to embrittlement of the samples. Stationary activity of the catalysts during the kinetic tests was confirmed by repetition of the first measurements after completion of the whole test series.

Conversion X [%] was defined as X = (moles CO_2 formed $\times$ 100)/(moles CO fed to the reactor). In all experiments reported the C-balance amounted to 100%.

RESULTS

Thermal Stability and Reactivity of Amorphous Pd_1Zr_2 in Different Gas Atmospheres

The crystallization behavior and the reactivity of the amorphous Pd_1Zr_2 alloy in the gas atmospheres used for the pretreatment of the precursor materials were investigated by differential thermal analysis (DTA), thermogravimetric analysis (TG), and X-ray diffraction (XRD).

The XRD patterns of the amorphous and crystalline Pd-Zr alloys used as catalyst precursors are presented in Fig. 1. The patterns of the amorphous sample show broad intensity maxima confirming the lack of long-range ordering of the constituents. The crystalline sample was prepared by annealing the amorphous alloy at 870 K in vacuum. The annealing led to the formation of crystalline Pd_1Zr_2 (*15*), as evidenced by XRD (Fig. 1).

Figure 2 shows the DTA and TG curves measured for the amorphous Pd_1Zr_2 alloy heated in Ar, N_2, CO, and O_2 atmospheres. Crystallization started at about 700 K (DTA curves) in argon, nitrogen, and CO atmospheres. In Ar and N_2 atmospheres no change in the sample weight was observed by TG. XRD indicated that the samples were crystalline after the DTA and TG measurements. The small increase in the sample weight at higher temperature in CO atmosphere was due to oxidation of zirconium by CO_2 and possibly the deposition of some carbon which had formed from CO under these conditions ($2CO \rightarrow CO_2 + C$). More complicated behavior was observed with amorphous Pd_1Zr_2 exposed to oxygen. Crystallization of the alloy started at significantly lower temperature and was accompanied by simultaneous oxidation as evidenced by XRD. The resulting solids were made up of monoclinic and tetragonal ZrO_2, Pd, and PdO.

Preparation of Active Catalysts from Palladium–Zirconium Alloy Precursors

The active catalysts were prepared in the fixed bed reactor from the amorphous and crystalline Pd_1Zr_2 alloys by exposing them to either CO oxidation conditions (in situ preparation) or to a continuous flow of air at a given temperature. Catalysts prepared from the amorphous precursor by in situ activation are referred to as *a-T, in situ* and those prepared by exposure to air as *a-T, air,* where *T* indicates the temperature (K) used. The crystalline precursor was also activated under CO oxidation conditions and is referred to as *c-T,* in situ.

Figure 3 shows the development of the CO-oxidation activity of the amorphous and crystalline precursors during their transformation to the active catalysts at different

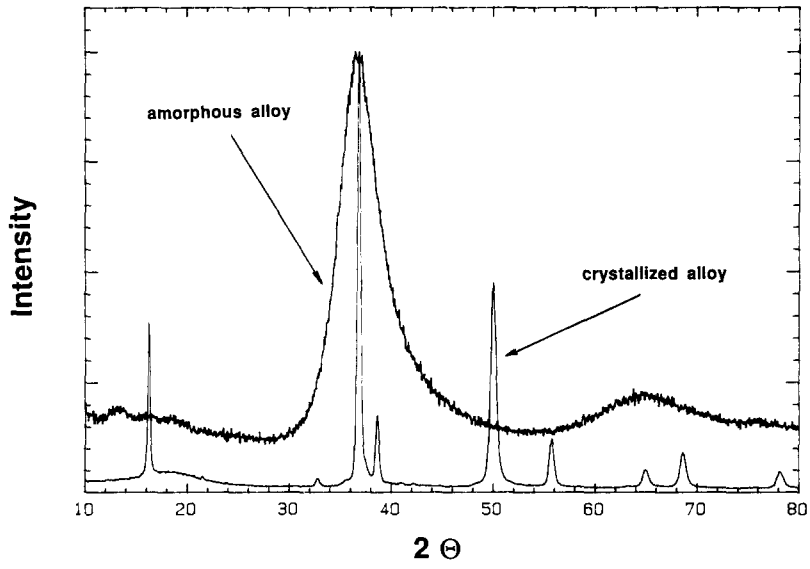

FIG. 1. X-ray diffraction patterns of amorphous and crystalline Pd_1Zr_2 alloys which were used as precursors. Cu$K\alpha$ radiation.

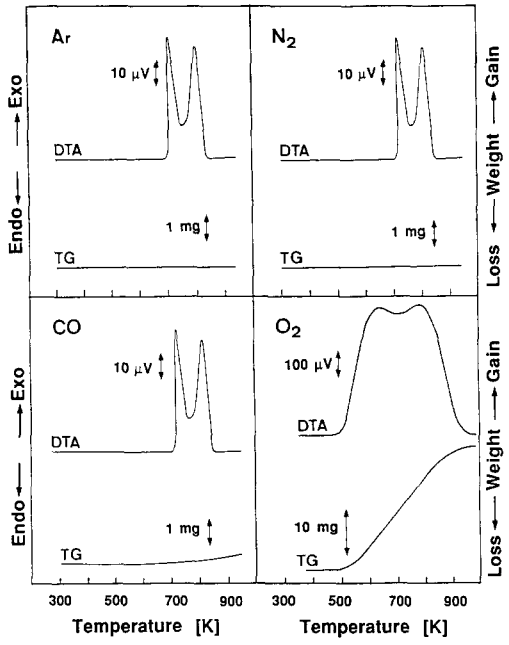

FIG. 2. Thermal stability and reactivity of amorphous Pd_1Zr_2 alloy in argon, nitrogen, carbon monoxide, and oxygen atmospheres investigated by DTA and TG. Heating rate 0.167 K/s.

conditions of *in situ* activation. Both precursors were virtually inactive at the start of the *in situ* activation. The activity developed with time on stream indicating that the exposure of the alloy to a CO/O_2 atmosphere or air at higher temperature was crucial for the preparation of active catalysts.

The development of the activity depended on the structure of the precursor and on

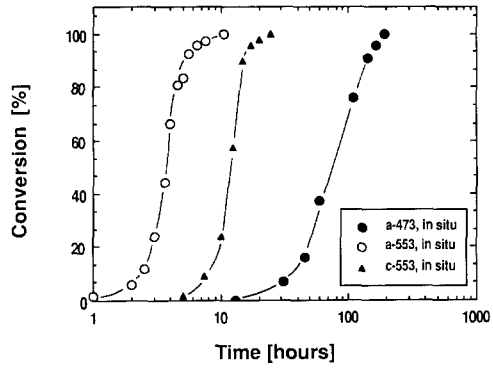

FIG. 3. CO oxidation activity of precursor materials as a function of time on stream. Conditions: catalyst load, 0.3 g; feed gas mixture CO, 0.17 kPa; O_2, 0.17 kPa; balance gas, N_2; total flow rate, 2.5 cm^3/s (STP); total pressure 100 kPa.

temperature. Lowering of the temperature slowed down markedly the development of the activity which is indicated by the shift of the curves shown in Fig. 3 to longer times on stream. Note that the crystalline precursor (c-553, in situ) showed a markedly slower development of the activity with time on stream compared to the similarly activated amorphous precursor (a-553, in situ). The time to reach steady-state activity increased in the sequence a-455 < a-513 < c-533 < a-473.

In a special series of experiments, the oxygen in the reactant feed was substituted by nitrogen after steady-state conversion was reached. It is noteworthy to mention that under these conditions the reaction proceeded for more than 20 min, indicating that a significant amount of oxygen was stored in the active catalyst.

Structural Changes of Amorphous and Crystalline Precursors During Exposure to Oxidation Conditions

The XRD patterns of the precursor (Fig. 1) and the active catalyst (Fig. 4, top) illustrate the bulk structural changes the amorphous Pd_1Zr_2 precursor underwent during in situ activation at 553 K. The diffraction patterns indicate that the precursor was transformed into a solid containing monoclinic and tetragonal ZrO_2, a solid solution of oxygen in Pd, metallic Pd, and PdO. The solid solution of Pd with oxygen is characterized by a shift of the main reflections of Pd toward lower 2θ. Both oxygen containing palladium phases disappeared slowly when the oxygen in the feed was substituted by nitrogen. Under these conditions the CO oxidation activity decreased slowly and after loss of the activity, the catalyst contained metallic Pd and monoclinic and tetragonal zirconia only.

Samples prepared under the same conditions starting from crystalline Pd_1Zr_2 showed similar behavior and similar phase compositions. However, the XRD reflections were less broadened due to the larger crystallite size of the constituents in these samples.

Figure 4 (bottom) depicts the XRD pattern of the Pd/ZrO_2 reference catalyst prepared by impregnation of zirconia with an aqueous solution of $(NH_4)_2PdCl_4$. This catalyst was made up predominantly of monoclinic ZrO_2 (baddeleyite) with tetragonal ZrO_2 and palladium as minor phases. Reflections of the palladium are not seen in the XRD pattern due to the low concentration of the metal (1% w/w). XRD line broadening and HREM (Fig. 8) indicated that the zirconia phase was made up of well crystalline particles of about 23 nm mean size.

Figure 5 shows CO adsorption isotherms measured for the active catalysts derived from the Pd_1Zr_2 alloy. The palladium metal surface areas derived from these measurements are listed together with the corresponding BET surface areas in Table 1. Measured nitrogen adsorption isotherms corresponded to type 1 according to the classification of Brunauer *et al.* (*16*).

The BET surface areas as well as the palladium surface areas increased by more than two orders of magnitude during the in situ activation of the Pd_1Zr_2 alloy. Depending on the conditions of the activation, the metal surface area (palladium) of the active catalysts was in the range 4–19 m^2/g, corresponding to a metal dispersion of 3 to 13%. Corresponding total surface areas of the active catalysts amounted to 24–46 m^2/g. The catalysts which were prepared by *in situ* activation of the amorphous precursor showed an increase in the total surface area and palladium surface area with increasing temperature. The largest palladium surface area was measured for the catalyst prepared from the amorphous precursor by pretreatment in air (a-553, air).

Nitrogen adsorption–desorption measurements performed on the solids derived from the amorphous and crystalline alloys indicated that these materials contained predominantly micropores. The *t*-plots (adsorbed volume versus statistical thickness of adsorbed layer) showed the characteristic

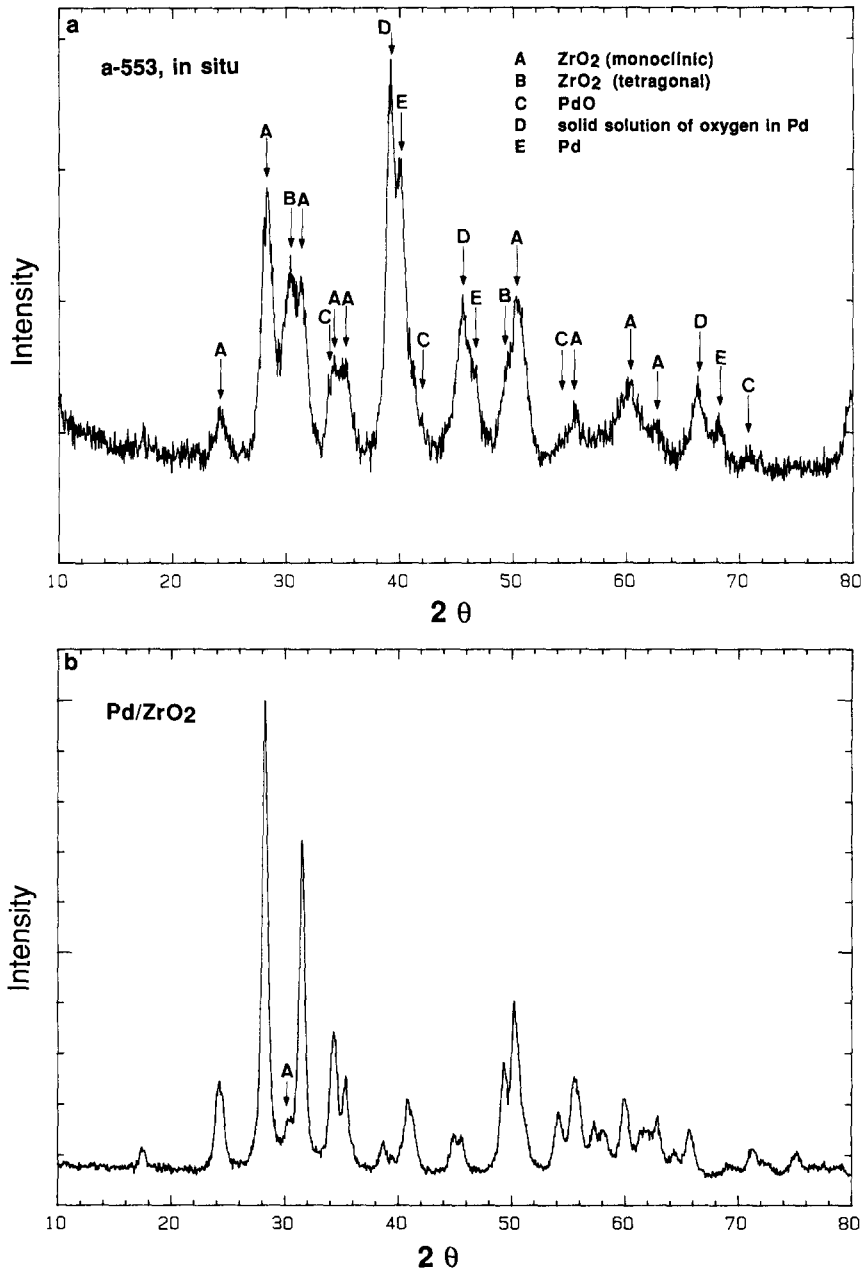

FIG. 4. X-ray diffraction patterns (Cu$K\alpha$) of catalysts derived from (a) amorphous Pd_1Zr_2 by *in situ* activation at 553 K and (b) reference catalyst Pd/ZrO_2 prepared by impregnation of zirconia with aqueous solution of $(NH_4)_2PdCl_4$ (palladium loading, 1 wt%).

deviation from linearity observed for microporous solids (*17*) and only very little hysteresis was observed between adsorption and desorption isotherms in the pressure range typical for mesopores.

The changes in the surface morphology of the amorphous precursor during its transformation to the active catalyst are illustrated by the scanning electron micrographs shown in Fig. 6. The initially flat surface

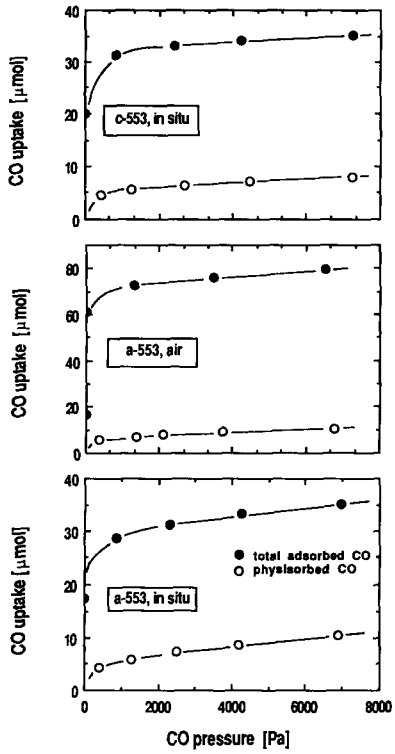

FIG. 5. CO adsorption isotherms measured for catalysts derived from amorphous and crystalline Pd_1Zr_2 alloys by *in situ* activation under CO oxidation conditions. Conditions of measurement are stated in experimental part.

of the precursor alloy changed to a rough surface which was built up of small agglomerates containing zirconia and palladium as evidenced by electron dispersive X-ray analysis.

High-resolution electron microscopy (HREM) as well as electron diffraction and optical diffraction of HREM images of the active catalyst showed that the aforementioned agglomerates (Fig. 7a) were made up of intimately mixed and intergrown small crystallites of zirconia and palladium species (Fig. 7b). The observed dimensions of the crystalline zirconia domains of 15–30 nm corroborate the mean domain size (23 nm) estimated by XRD line broadening. Note that the micromorphology of the zirconia crystallites is irregular leading to an extremely large interfacial area between the zirconia and palladium phases. As indicated by the rather diffuse reflections in the electron diffraction pattern (Fig. 7b, inset) the poorly crystalline domains of the palladium species are fully integrated into zirconia. The absence of well-developed crystallites of any palladium species provides further evidence that these compounds are fully integrated in the zirconia matrix and that they adopt irregular micromorphologies with high interfacial areas.

Similar structural and morphological features were observed for samples obtained from crystalline Pd_1Zr_2 precursors. However, the crystalline domain sizes of the constituents were considerably larger, and accordingly, the interfacial area is expected to be smaller in these samples.

For comparison, the conventionally prepared Pd/zirconia catalysts were also investigated using HREM. Figure 8a depicts an overview illustrating the textural features of such a catalyst. Even at this relatively low magnification, the well-developed crystallites of the constituents are visible and exhibit a regular morphology (ball-shaped). This feature was found to be typical for all palladium on zirconia catalysts prepared by impregnation of zirconia with a palladium salt. Owing to this particular morphology originating from the poor contact (wetting) of the metal with the zirconia support, the interfacial area between these phases is comparatively small in as-prepared catalysts. Experimental evidence for this behav-

TABLE 1

BET and CO Chemisorption Measurements of Investigated Catalysts

Catalyst	Surface area BET (m^2/g)	Palladium surface area (m^2/g)	Dispersion (%)
Amorphous Pd_1Zr_2	0.03		
Crystalline Pd_1Zr_2	0.05		
a-473, *in situ*	26.9	3.9	2.7
a-553, *in situ*	45.9	6.9	5.9
a-553, air	24.2	18.5	13.2
c-553, *in situ*	20.2	6.9	5.1
1% Pd/ZrO_2	45.5	0.5	11.6

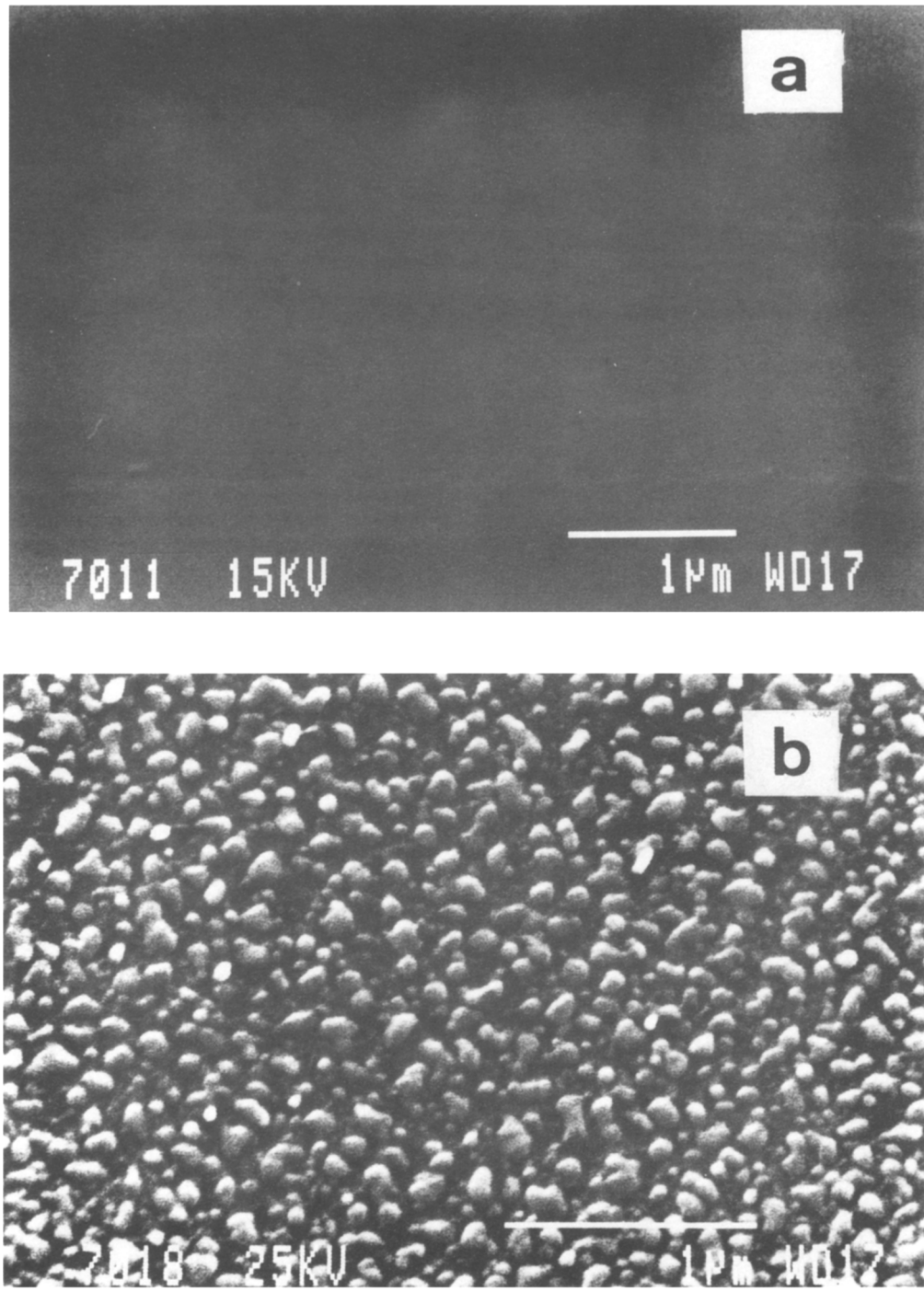

FIG. 6. Scanning electron micrographs showing the change in the surface morphology of the amorphous Pd_1Zr_2 alloy after *in situ* activation at 553 K. (a) Amorphous alloy precursor; (b) catalyst after steady-state activity was reached.

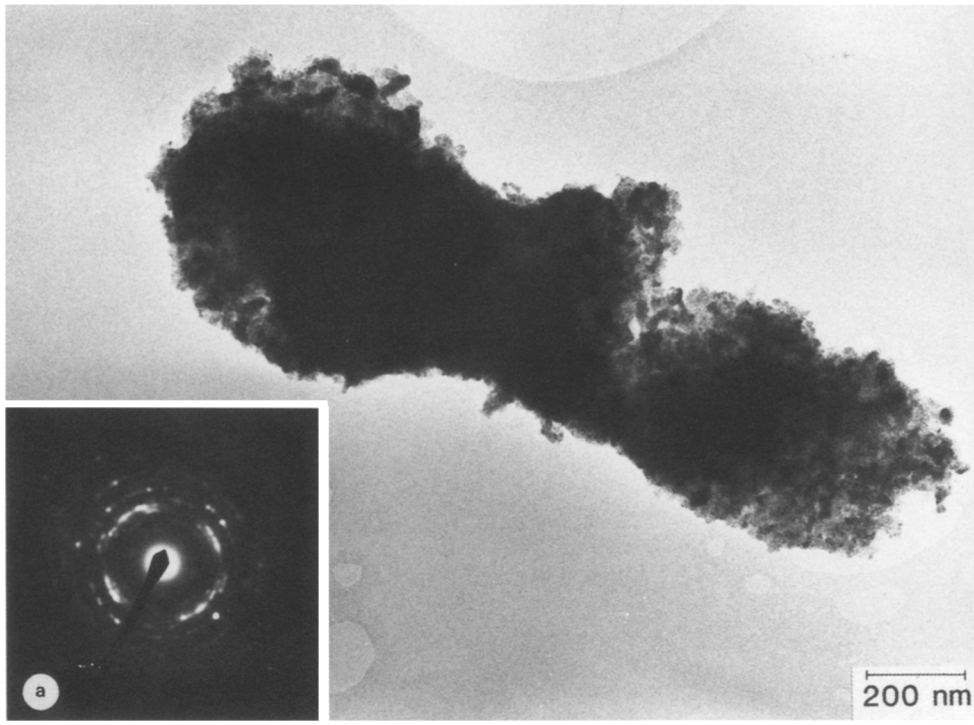

FIG. 7. Morphology and structure of the active catalyst prepared from the amorphous Pd_1Zr_2 alloy by *in situ* activation at 553 K. (a) Electron micrograph and electron diffraction pattern of a flake of the active catalyst. (b) High-resolution electron micrograph and electron diffraction pattern of an area of the active catalyst. The presence of intimately mixed and intergrown crystalline domains of zirconia and palladium species is observed. The domain sizes of the primary crystallites are in the range of 10–30 nm. The arrows in the electron diffraction pattern indicate the rather diffuse reflections originating from the Pd species.

ior emerged from investigations by means of HREM and optical diffraction techniques (Fig. 8b) which showed that in the conventionally prepared catalysts zirconia is present as crystallites with dimensions in the range well above 30 nm. Palladium forms well-developed "single crystallites" with regular micromorphologies, as HREM imaging and optical diffraction of isolated palladium particles (see inset Fig. 8b) revealed.

Catalytic Behavior of the Stable Active Catalysts

Figure 9 compares CO conversions measured at various temperatures over the differently prepared catalysts after steady-state reaction rates were reached. Note that the overall activity of the resulting catalysts depended on the pretreatment. Catalysts prepared from amorphous Pd_1Zr_2 by *in situ* activation or activation in air at 553 K were most active. With the amorphous Pd_1Zr_2, there was a clear tendency for the overall activity to increase with increasing activation temperature. The catalyst prepared by impregnation exhibited by far the lowest activity. It is important to note that the pure support material (ZrO_2) did not exhibit significant activity for CO oxidation under the conditions used.

The specific activities of the catalysts were determined as turnover frequencies (TOF) based on the assumption that Pd is part of the active species. The kinetic results are presented as Arrhenius plots in Fig. 10. Turnover frequencies were calculated from

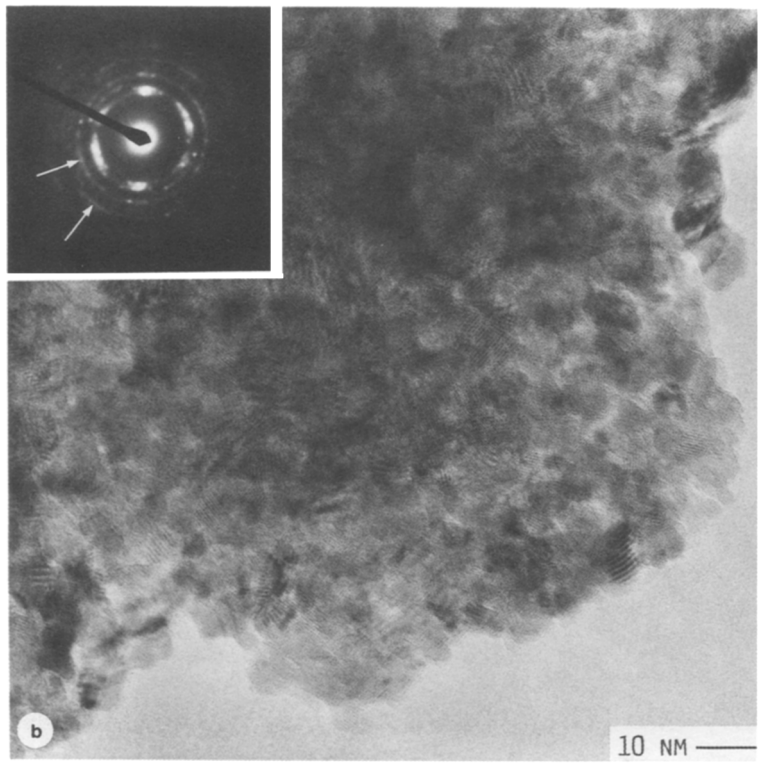

FIG. 7—*Continued*

differential reactor experiments using the relation $r[\mathrm{TOF}] = F/\mathrm{Pd_s}$, where F is the molar flow rate of CO_2 leaving the reactor, and $\mathrm{Pd_S}$ the number of palladium surface metal atoms in the catalyst bed. The apparent activation energies (kJ/mol) derived from these measurements were: a-473, 36.1 ± 1; a-553, 26.2 ± 1; a-553/air, 27.9 ± 1; c-553, 28.1 ± 1; $\mathrm{Pd/ZrO_2}$, 54.8 ± 1.

Note that the $\mathrm{Pd/ZrO_2}$ catalyst prepared by wet impregnation exhibited an activation energy about two times higher than the catalysts prepared from $\mathrm{Pd_1Zr_2}$. Activation at higher temperature improved both the overall activity and the turnover frequency of the catalysts prepared from amorphous $\mathrm{Pd_1Zr_2}$. The highest turnover frequency was observed with catalyst a-553, *in situ*. However, the overall activity of catalyst a-553, air was about the same as that of catalyst a-553, *in situ* (Fig. 10), due to the higher palladium dispersion of catalyst a-553, air.

DISCUSSION

Genesis of Active Catalysts from Metal Alloy Precursor

Figure 11 shows schematically the chemical transformations of the metal alloy precursors during *in situ* activation and after the oxygen supply was stopped during CO-oxidation. Exposure of $\mathrm{Pd_1Zr_2}$ to a pure CO atmosphere did not lead to marked changes of the bulk structure of the precursor, i.e., the presence of oxygen was crucial.

The working catalyst contains palladium in three different forms: as solid solution with oxygen, as metal, and as palladium oxide (PdO). The concentrations of these phases depends on the degree of oxidation of the alloy, i.e., on the content of metallic zirconium in the sample. It has been evidenced in a separate study (*18*) that the presence of metallic zirconium largely influences the concentrations of these phases. Zirco-

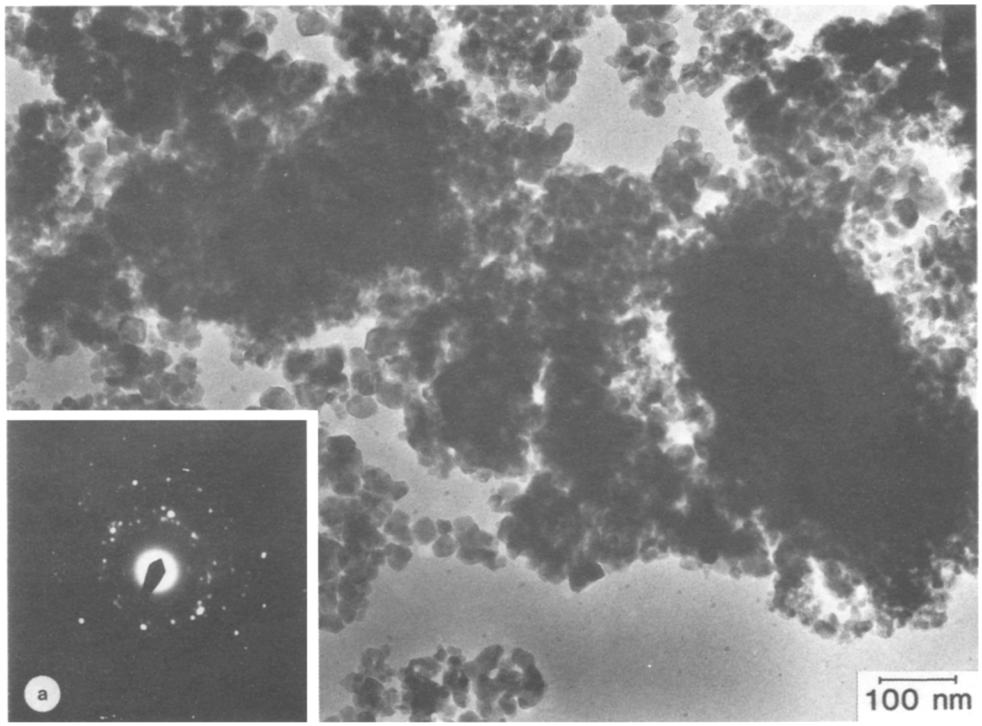

FIG. 8. Morphology and structure of conventionally prepared palladium on zirconia catalyst (metal loading 5%). (a) Electron micrograph showing an overview on the texture of the catalyst. (b) High-resolution electron micrograph and electron diffraction pattern of the catalyst. The zirconia crystallites with diameter above 30 nm and the well-developed palladium crystallites with diameters in the range 10–30 nm are clearly visible. The electron diffraction pattern gives evidence for the presence of only well crystallized species. As inset a typical palladium "single crystallite" with the corresponding optical diffraction pattern is shown.

nium was found to reduce the PdO formed by oxidation of Pd with gaseous oxygen supplied in the reactant feed. The reduction of PdO by zirconium occurs simultaneously under in situ activation conditions and lowers the PdO concentration. The concentration of PdO is therefore expected to increase with decreasing content of the metallic zirconium in the sample.

The formation of a solid solution of the palladium with oxygen has, to our knowledge, hitherto not been reported for Pd–Zr alloys. While the chemical nature of oxygen adsorbed on palladium and bulk crystalline PdO are rather well understood, the intermediate palladium/oxygen phases are still a matter of controversy. It is not clear whether this state should be described as a solid solution of oxygen in Pd, as proposed by Campbell *et al.* (*19*), or as some kind of "subsurface oxide" (*20, 21*). Peuckert (*22*) suggested that such intermediate phases could be regarded as structures either containing small metal clusters imbedded in an oxide matrix or oxide clusters enclosed in reduced metal. It is noteworthy that the formation of a solid solution was not observed if the alloy was pretreated in oxygen or air at the same temperature. Under these conditions only zirconia, metallic palladium, and PdO were found by XRD. This behavior indicates that the limitation of the oxygen

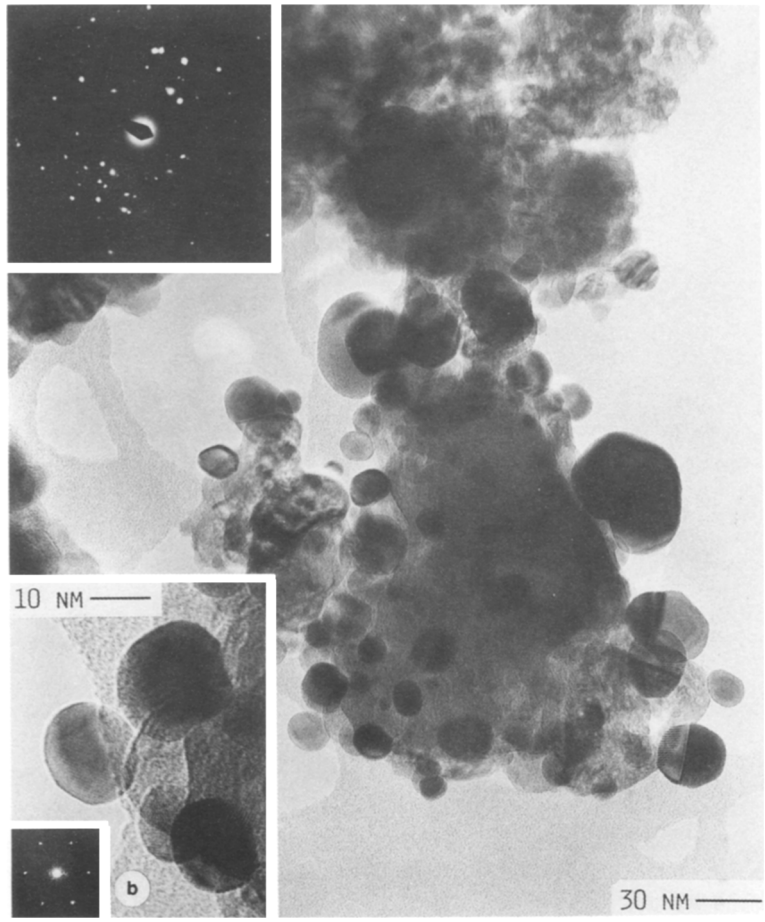

FIG. 8—*Continued*

supply is crucial for the formation of the solid solution. During *in situ* activation conditions the oxygen supplied by the reactant feed is consumed mainly by the oxidation of zirconium to zirconium oxide and the simultaneously occurring CO-oxidation; i.e., conditions of limited oxygen supply are governing.

The formation of the solid solution could be viewed to be an intermediate step of the solid state reduction $2PdO + Zr \rightarrow \{2(Pd + O) + Zr\} \rightarrow 2Pd + ZrO_2$. In any case, there is no doubt that the complex interplay between the solid state reduction of PdO by zirconium, the removal of oxygen by the CO-oxidation, and the oxidation of Pd by the gaseous oxygen supplied by the reactant feed determines the distribution of the different palladium phases observed.

Zirconia was found to adopt the monoclinic and tetragonal structure in the active catalysts derived from the amorphous and crystalline metal alloys. X-ray photoelectron spectroscopy indicated that in the surface and subsurface region zirconia exists as non-stoichiometric ZrO_{2-x}, as will be shown in part 2 of this work (*8*). The presence of nonstoichiometric ZrO_{2-x} has also been observed in oxidized Ni–Zr alloys (*23–25*). In contrast, the zirconia support

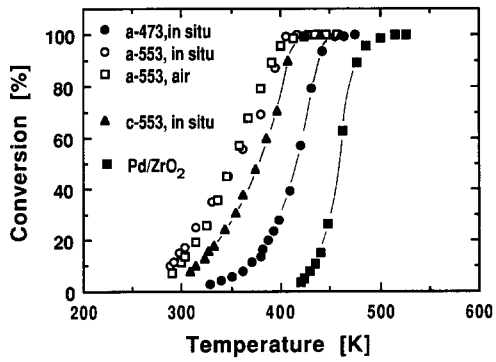

FIG. 9. Influence of temperature on CO conversion measured for different catalysts. Pd/ZrO_2 represents conventionally prepared Pd on zirconia catalyst. Conditions: catalyst load, 0.3 g; feed gas mixture CO, 0.17 kPa; O_2, 0.17 kPa; balance gas, N_2; total flow rate, 2.5 cm^3/s (STP); pressure 100 kPa.

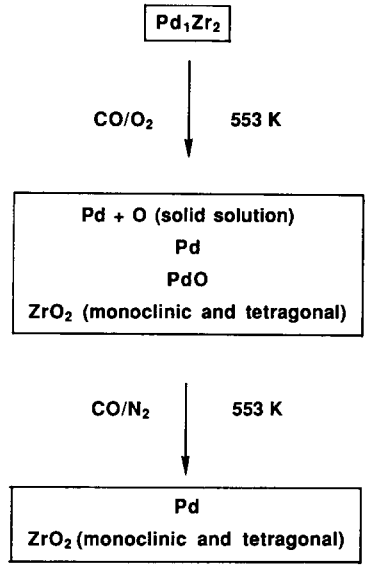

FIG. 11. Chemical transformations of the Pd_1Zr_2 alloys during exposure to CO oxidation conditions. Corresponding conversion versus time curves are shown in Fig. 3.

of the conventionally prepared catalyst was made up of well-crystalline monoclinic ZrO_2.

Another striking difference between the bulk structure of the catalyst prepared from Pd_1Zr_2 and that of the reference catalyst (Pd/ZrO_2) lies in the particle size of their constituents. High-resolution electron microscopy (Fig. 7) as well as XRD (Fig. 4a) indicated that the catalysts prepared from Pd_1Zr_2 were made up of intergrown small and poorly crystalline particles, which form an extremely large interfacial area between the metal and oxide phases. Conversely the typical structure of conventionally prepared Pd/ZrO_2 (Fig. 8) is characterized by a relatively low interfacial area between metal and oxidic support. Figure 12 illustrates schematically the morphological build-up of the active catalysts derived from the Pd_1Zr_2 alloys.

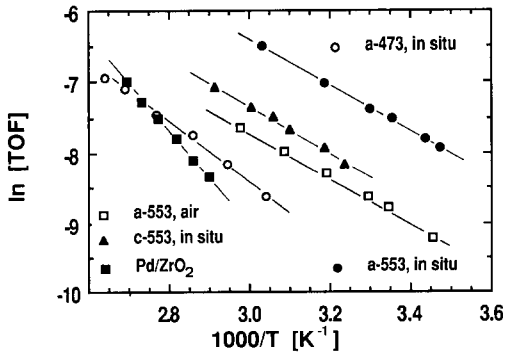

FIG. 10. Comparative study of catalyst activities. Turnover frequencies measured for CO oxidation over different catalysts. Arrhenius plots are presented. For conditions see Fig. 9.

It is interesting to note that efficient catalysts could be prepared from amorphous as well as from crystalline Pd_1Zr_2. The active catalysts showed similar phase composition; however, the crystalline domain sizes of the constituents were significantly larger, resulting in a considerably lower interfacial area beween metal and oxide phases. In addition, the transformation of the crystalline precursor to the active catalyst was considerably slower compared to the one of the amorphous precursor. This behavior stands in contrast to the behavior observed for copper–zirconium alloys (*26, 27*), where amorphous precursor alloys were necessary to prepare efficient supported metal catalysts.

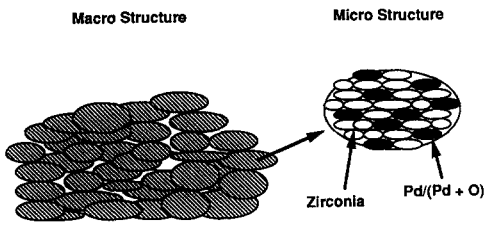

FIG. 12. Schematic illustration of morphological and structural characteristics of the catalyst prepared from the amorphous Pd_1Zr_2 alloy by *in situ* activation. Note that the shape of the particles which built up the microstructural units is much more irregular than shown in this illustration.

Catalytic Behavior of Catalysts Derived from Metal Alloys

The catalytic tests (Fig. 3) showed that amorphous and crystalline Pd_1Zr_2 in as-prepared states are virtually inactive for CO oxidation. This is attributed to the small surface area of the precursors (0.03 m^2/g) and the presence of a stable zirconium oxide layer covering the surface of the freshly prepared ribbons (*24, 28*). Exposure of the alloys to CO oxidation conditions or to an oxygen-containing atmosphere at elevated temperature produces catalysts which exhibit excellent activity for CO oxidation. Drastic changes of the bulk and surface structure of the amorphous and crystalline alloys are responsible for the activity increase.

The oxidation of carbon monoxide over palladium was shown to be structure-insensitive in several investigations (*1, 29*). The present investigations indicate that structural differences in both the active metal species and the zirconia support are the main reason for the observed differences in the activity of the two palladium/zirconia catalysts.

As regards the markedly lower apparent activation energies of the catalysts derived from the metal alloys, two possible reasons have to be considered, namely mass transfer control by intraparticle diffusion in the microporous solids or the different nature of the active sites. Our experiments do not allow us to discriminate between these two influences, since mass transfer control in the micropores cannot be ruled out. In fact, assuming a first-order reaction in CO, we would expect that the apparent activation energy of the microporous catalysts derived from the metal alloys would be half of the activation energy of the conventionally prepared catalyst, where diffusional restrictions could be ruled out as was evidenced by a series of measurements with catalysts of different particle size. In view of this, the turnover frequencies determined for the catalysts derived from the metal alloys have to be considered as conservative estimates, probably influenced by intraparticle mass transfer limitation.

As concerns the influence on the apparent activation energy by the different nature of the active sites. Yung-Fang Yu Yao (*30*) made a detailed study of the kinetic parameters for the oxidation of CO over Pt, Pd, and Rh. The metals were used in the form of unsupported wires or as particles supported on γ-Al_2O_3 or CeO_2/Al_2O_3. The author postulated two types of surface sites each with its own reaction kinetics to explain the kinetic results.

Type 1 kinetics, exemplified by the precious metal (PM) wires, is first-order with respect to O_2 and negative first-order with respect to CO. These sites were attributed to PM particles in low oxidation state. Type 2 kinetics is of positive order with respect to CO and nearly independent of the oxygen partial pressure. This type of kinetics prevailed over PM surfaces of higher dispersion and higher oxidation state. In essence, the active type 2 sites present as cations would be surrounded by oxygen either as ions or as adsorbed oxygen species. The activation energies in type 2 kinetics were found to be generally lower. It is interesting to note that the catalysts derived from the metal alloys showed a qualitative behavior similar to the type 2 kinetics suggested in Ref. (*30*).

Our comparative kinetic studies indicate

that the intrinsic activity of palladium species in a palladium-on-zirconia catalyst prepared by *in situ* oxidation of an amorphous or crystalline Pd_1Zr_2 alloy is markedly higher than that of palladium species in a Pd/ZrO_2 catalyst prepared by impregnation. Drastic differences in the morphological and chemical properties of these catalysts are the reason for the different CO-oxidation activity observed. The catalysts derived from the metal alloys are made up of small intergrown crystalline domains of palladium phases (Pd + O, Pd, PdO) and nonstoichiometric zirconia forming an extremely large interfacial area. It is suggested that these structural features facilitate the transfer of oxygen through the ion conducting zirconia to the active palladium phase and thereby enhance the CO-oxidation rate. A similar oxygen transfer is not feasible for the structure of the conventionally prepared Pd/ZrO_2 catalyst. Further support for this explanation will be shown in Part 2 (*8*) of this work, where *in situ* studies of the surface properties of the catalysts derived from the metal alloys will be addressed.

CONCLUSIONS

Amorphous and crystalline Pd_1Zr_2 alloys are shown to be interesting precursors for the preparation of active CO-oxidation catalysts. The stable catalysts were prepared by oxidizing the metal alloys *in situ*, i.e., under CO-oxidation conditions at 473, 513, and 553 K. Under these conditions the initially almost inactive metal alloys transformed to highly active microporous CO-oxidation catalysts which consisted of intergrown small and poorly crystalline domains of palladium and zirconia phases. Three different palladium phases were discernable by XRD, a solid solution of palladium with oxygen, Pd, and in smaller amount, PdO. The palladium phases were homogeneously distributed in a zirconia matrix made up of monoclinic and tetragonal ZrO_2.

The CO-oxidation activities of the catalysts prepared from the metal alloys were measured as turnover frequencies (TOF) in the temperature range 300–500K and compared to a conventionally prepared palladium-on-zirconia catalyst. The activity of the palladium species in the catalyst derived by oxidation of amorphous Pd_1Zr_2 was more than an order of magnitude higher than the activity of the palladium species in the conventionally prepared catalyst. This behavior is attributed to the particular morphological and structural properties of the catalysts derived from the metal alloys, which are suggested to facilitate oxygen transfer through the zirconia/palladium interphase.

ACKNOWLEDGMENTS

Thanks are due to K. Heinzen for preparing the metal alloys, to P. Wägli for the SEM investigation, and to Dr. M. Maciejewski for his help with the thermoanalytical investigations. Financial support of this work by LONZA AG, Switzerland, and the Swiss National Science Foundation is kindly acknowledged.

REFERENCES

1. Engel, T., and Ertl, G., *Adv. Catal.* **28,** 1 (1979).
2. Yoon, C., and Cocke, D. L., *J. Non-Cryst. Solids* **79,** 217 (1986).
3. Molnar, A., Smith, G. V., and Bartok, M., *Adv. Catal.* **36,** 329 (1989).
4. Baiker, A., *Faraday Discuss. Chem. Soc.* **87,** 239 (1989).
5. Maciejewski, M., and Baiker, A., *J. Chem. Soc. Faraday Trans.* **86,** 843, (1990), and references therein.
6. Shibata, M., and Masumoto, T., *Stud. Surf. Sci. Catal.* **31,** 353 (1987).
7. Baiker, A., Gasser, D., and Lenzner, J., *J. Chem. Soc. Chem. Commun.*, 1750 (1987).
8. Schlögl, R., Lohse, G., Wesemann, M., and Baiker, A., manuscript in preparation.
9. ASTM Powder Diffraction File 13-307, Joint Committee on Powder Diffraction Standards, Pennsylvania, 1979; Lewis, General Electric Co., ANP DEPT., Cincinatti 15, Ohio.
10. Joyal, C. L. M., and Butt, J. B., *J. Chem. Soc. Faraday Trans. 1* **83,** 2757 (1987).
11. Ichikawa, S., Poppa, H., and Boudart, M., *J. Catal.* **91,** 1 (1985).
12. Barnickel, P., Wokaun, A., and Baiker, A., *J. Chem. Soc. Faraday Trans.*, in press.
13. Anderson, J. R., and Pratt, K. C., "Introduction to Characterization and Testing of Catalysts," p. 268, Academic Press, London, 1985.
14. Rau, R. C., in "Encyclopedia of X-Rays and γ-Rays" (G. L. Clark Ed.), p. 184, Reinhold, New York, 1963.

15. ASTM Powder diffraction File 18-1962, ed. Joint Committee on Powder Diffraction Standards, Pennsylvania, 1979; Nevitt, M. V., and Downey, J. W., private communication, 1966.
16. Brunauer, S., Deming, L. S., Deming, W. E., and Teller, E., *J. Amer. Chem. Soc.* **62,** 1723 (1940).
17. Lecloux, A. J., *in* "Catalysis, Science and Technology" (J. R. Anderson and M. Boudart, Eds.), Vol. 2, p. 172, Springer-Verlag, Berlin, 1981.
18. Maciejewski, M., and Baiker, A., manuscript in preparation.
19. Campbell, C. T., Foyt, D. C., and White, J. M., *J. Phys. Chem.* **81,** 491 (1977).
20. Conrad, H., Ertl, G., Küppers, J., and Latta, E. E., *Surf. Sci.* **65,** 245 (1977).
21. Legaree, P., Hilaire, L., Maire, G., Krill, G., and Amamou, A., *Surf. Sci.* **107,** 533 (1981).
22. Peuckert, M., *J. Phys. Chem.* **89,** 2481 (1985).
23. Armbruster, E., Baiker, A., Güntherodt, H. J., Schlögl, R., and Walz, B., *Stud. Surf. Sci. Catal.* **31** (*Prep. Catal.* 4), 389 (1987).
24. Walz, B., Oelhafen, P., Güntherodt, H. J., and Baiker, A., *Appl. Surf. Sci.* **37,** 337 (1990).
25. Baiker, A., De Pietro, J., Maciejewski, M., and Walz, B., *Prepr. Amer. Chem. Soc. Div. Pet. Chem.* **35,** 79 (1990).
26. Baiker, A., Baris, H., and Güntherodt, H. J., *J. Chem. Soc. Chem. Commun.*, 930 (1986).
27. Gasser, D., and Baiker, A., *Appl. Catal.* **48,** 279 (1989).
28. Vanini, F., Büchler, S., Xin-nan Yu, Erbudak, M., Schlappach, L., and Baiker, A., *Surf. Sci.* **189/190,** 1117 (1987).
29. Ladas, S., Poppa, H., and Boudart, M., *Surf. Sci.* **102,** 151 (1981).
30. Yu Yao, Y. F., *J. Catal.* **28,** 1 (1979).